The Structure of Liquid Copper-Magnesium Alloys*

W. E. LUKENS** and C. N. J. WAGNER

Becton Center, Yale University, New Haven, Connecticut 06520

Materials Department, School of Engineering and Applied Science, University of California, Los Angeles

(Z. Naturforsch. **28 a**, 297–304 [1973]; received 20 Novembre 1972)

X-rays (MoKα) have been used as a radiation probe to evaluate the interference functions $I(K)$ (or structure factors) of liquid Cu, Mg and Cu-Mg alloys with 49, 66, and 86 at. % Mg at temperatures about 50 °C above the liquidus. Employing the transmission technique, $I(K)$ has been determined in the range of $K = 4\pi \sin\Theta/\lambda$ between 0.8 A^{-1} and 12.5 A^{-1}. All $I(K)$ of the alloys exhibit a premaximum at $K = 1.5$ A^{-1}.

The partial interference functions $I_{ij}(K)$ have been determined, and it was found that the assumption of concentration independence of $I_{ij}(K)$ yielded reduced partial distribution functions $G_{ij}(r)$, the weighted sum of which were only in fair agreement with $G(r)$, the Fourier transform of $F(K) = K[I(K)-1]$.

The positions, r, of the first peak in $G(r)$ and the coordination number, η, determined from the radial distribution function $4\pi r^2 \varrho(r) = r\,G(r) + 4\pi r^2 \varrho_0$, where ϱ_0 is the average atomic density of the alloy, show a negative deviation from a straight line when plotted as a function of concentration, which might be considered as evidence for the existence of short-range order in the liquid. Art. 2288

I. Introduction

The vast majority of pure liquid metals and binary alloys of liquid metals are characterized by total interference functions ($I(K)$, which show a relatively strong first peak, representative of interference occurring between nearest neighbors[1]. The presence of a weak peak at a smaller K value than that of the first peak might be due to the occurrence of interference between atoms whose distance of separation is somewhat greater that of the first nearest neighbors. The presence of such a „premaximum" was observed in the $I(K)$ of liquid Ag-Mg alloys as early as 1966 by STEEB and HEZEL[2]. Other Mg-base alloys, i.e., Al-Mg[3], Mg-Sn[4], Mg-Pb[5] and Cd-Mg[6], had been investigated previously and some of these also exhibited the presence of a premaximum. The investigation reported herein was performed to obtain data on yet another Mg-base alloy, i.e., Cu-Mg with a view toward determining common factors in these alloy systems which might be responsible for this premaximum.

The atomic arrangements in liquids must be deduced from the entire intensity distribution of the scattered X-rays or neutrons. This condition arises from the fact that in these structures there are no Bragg peaks, which result from long-range atomic order. Therefore, a simple separation into peaks and background is not possible. The intensity of elastically scattered X-rays from a sample can be interpreted in terms of the atomic distribution functions, $\varrho_{ij}(\vec{r})$, (which specify the number of j-type atoms per unit volume at the directional distance $\vec{r}$ from an i-type atom). A simplifying assumption is made that the atomic distributions in liquid structures are spherically symmetrical. This assumption provides the basis for considering $\varrho_{ij}(r)$ as a function of radial distance only.

The total radiation scattered from a specimen consists of two components. There is the small-angle scattering component which is close to the primary beam, and the large angle scattering component which includes scattering at all other angles. In this investigation data were obtained using only large angle scattering, which is dependent on $\varrho_{ij}(r)$ and the size of the coherently diffraction domain.

The total scattered intensity per atom, $I_a(K)$, can be written as

$$I_a(K) = \langle f^2\rangle - \langle f\rangle^2 + \langle f\rangle^2 I(K) \qquad (1)$$

where $\langle f\rangle$ and $\langle f^2\rangle$ are the mean and the mean square scattering factors. $I(K)$ represents the large angle diffraction, and can be expressed for isotropic and macroscopically homogeneous materials as [1]

$$I(K) = 1 + \int_0^\infty 4\pi r^2 [\varrho(r) - \varrho_0]\, V(r)\, (\sin Kr/Kr)\, dr \qquad (2)$$

* Research supported by the U.S. Atomic Energy Commission

** Present address: Naval Ship Research and Development Center, Annapolis, Maryland 21402.

Reprint requests to: Prof. Dr. C. N. J. WAGNER, Materials Department, School of Engineering and Applied Science, University of California, *Los Angeles*, Calif. 90024, U.S.A.

where $\varrho(r)$ is the weighted atomic distribution function, $V(r)$ is the size factor of coherently diffracting domains and ϱ_0 is the macroscopic atomic density of the material. In liquids, the assumption that $V(r) = 1$ is made for standard sample sizes [$>$ (1000 Å)^3]. $I(K)$ can also be represented as a sum of the partial interference function $I_{ij}(K)$[1,7,8].

$$I(K) = \sum_i \sum_j c_i\, c_j\, (f_i f_j^*/\langle f\rangle^2)\, I_{ij}(K) \tag{3}$$

where

$$I_{ij}(K) = \tag{4}$$
$$= 1 + \int_0^\infty 4\pi r^2 [(\varrho_{ij}(r)/c_j) - \varrho_0] (\sin Kr/Kr)\, \mathrm{d}r = I_{ji}(K)$$

and c_i is the atomic concentration of i-type atoms. For large values of r, $\varrho_{ij}(r)$ tends towards $c_j \varrho_0$, or $\varrho_{ij}(r)/(c_j \varrho_0) \to 1$. Therefore, one may define a pair distribution or probability function $g_{ij}(r)$:

$$g_{ij}(r) = (\varrho_{ij}(r)/c_j \varrho_0)\,. \tag{5}$$

The Fourier transforms of the reduced partial interference functions $K[I_{ij}(K) - 1]$ yield the reduced partial distribution functions $G_{ij}(r)$:

$$\begin{aligned} G_{ij}(r) &= 4\pi r \varrho_0 [g_{ij}(r) - 1] = \\ &= (2/\pi) \int_0^\infty K [I_{ij}(K) - 1] \sin Kr\, \mathrm{d}K \end{aligned} \tag{6}$$

and in analogy, the Fourier transform of the reduced total interference function $K[I(K) - 1]$ yields the reduced total distribution function $G(r)$:

$$\begin{aligned} G(r) &= 4\pi r [\varrho(r) - \varrho_0] = \\ &= (2/\pi) \int_0^\infty K [I(K) - 1] \sin Kr\, dK. \end{aligned} \tag{7}$$

It can be shown[1,9] that $G(r)$ is the convolution product of $G_{ij}(r)$ and $W_{ij}(r)$; i.e.,

$$G(r) = \sum_i \sum_j W_{ij}(r)^*\, G_{ij}(r) \tag{8}$$

where

$$W_{ij}(r) = (1/\pi) \int_0^\infty w_{ij}(K) \cos Kr\, \mathrm{d}K \tag{9}$$

and

$$w_{ij}(K) = c_i\, c_j (f_i f_j^*/\langle f\rangle^2). \tag{10}$$

If $w_{ij}(K)$ is independent of K, then Eq. (9) can be simplified to

$$W_{ij}(r) = w_{ij}\delta(r).$$

Equation (8) then reduces to

$$G(r) = \sum_i \sum_j w_{ij} G_{ij}(r)\,. \tag{11}$$

From this expression it follows immediately that[10]

$$\varrho(r) = \varrho_0 \sum_i \sum_j w_{ij}\, (\varrho_{ij}(r)/c_j \varrho_0) \tag{12}$$

or

$$g(r) = \sum_i \sum_j w_{ij}\, g_{ij}(r), \tag{13}$$

where $g(r) = \varrho(r)/\varrho_0$ is the total pair distrubution function.

It must be emphasized that Eq. (12) is based on the assumption that w_{ij} is independent of K, an assumption which is well fulfilled in neutron scattering. The consequence of assuming w_{ij} to be constant in X-ray scattering experiments has been discussed by PINGS and WASER[9], and KAPLOW, STRONG and AVERBACH[10]. It has been shown that in the $G(r)$ curves, there is a possibility that the convolution of $G_{ij}(r)$ with $W_{ij}(r)$ will sharpen $G(r)$ by slightly incorrent amounts, leaving some parts too broad and making others too sharp.

The radial distribution function is defined as the number of atoms in a spherical shell of radius r and thickness unity; i.e., $4\pi r^2 \varrho(r)$. It follows from Eq. (7) that

$$4\pi r^2 \varrho(r) = rG(r) + 4\pi r^2 \varrho_0. \tag{14}$$

As can be seen from Eq. (7), $G(r)$ depends on $\varrho(r)$. $G(r)$ becomes zero when $\varrho(r) - \varrho_0$ becomes zero; i.e., beyond a certain distance r_s, $\varrho(r) \sim \varrho_0$.

For binary alloys, $I(K)$ [Eq. (3)] reduces to

$$I(K) = w_{11} I_{11}(K) + 2 w_{12} I_{12}(K) + w_{22} I_{22}(K). \tag{15}$$

We see here that there are three partial interference functions $I_{11}(K)$, $I_{12}(K)$ and $I_{22}(K)$ to be determined. A complete analysis of a binary alloy, therefore, requires a minimum of three separate diffraction experiments utilizing radiations which yield different ratios between f_1 and f_2. This would permit one to obtain $I_{11}(K)$, $I_{12}(K)$ and $I_{22}(K)$ by a simultaneous solution of three equations like Eq. (15). This can be best accomplished by isotope enrichment of the elements and subsequent measurement of the neutron scattering from the sample, a method suggested by KEATING and applied be ENDERBY, NORTH and EGELSTAFF[12] to liquid Cu_6Sn_5.

If $I_{ij}(K)$ are independent of c_i, one can determine them by varying c_i in Equation (3). This method has been applied to the liquid Ag-Sn[13], Au-Sn[14], Ag-Mg[15] and Cu-Sn[16] alloy systems.

II. Experimental Technique

A) X-Ray Technique

All data were taken in the transmission mode of operation using a Siemens diffractometer, which has been described befor by NORTH and WAGNER[17]. X-rays from a line source (molybdenum target) impinged on a flat graphite monochromator. The horizontal divergence of the beam was defined by an array of slits. The sample rotated at half the angular speed of the X-ray detector.

Detection of the diffracted intensity was made by a scintillation counter coupled to an amplification system, scaler and print-out system. The step-scan mode of operation was used.

A furnace assembly of NORTH and WAGNER[17] has been modified for the studies of liquid Mg-Cu alloys. The furnace consisted of a graphite tube (0.025″ (0.64 mm) wall-thickness and 1.5″ (38 mm) diameter) whose height was increased to 7″ (180 mm) and into which slits were machined diametrically opposite each other to within 0.75″ (19 mm) of one end, thus forming a quasi-cylinder. The increased height insured a more uniform temperature distribution in the sample. Thermocouple output was recorded on a Leeds and Northrup Speedomax H Recorder, and the temperature was controlled by a Leeds and Northrup CAT control unit and silicon controlled rectified power package.

The camera housing, which enclosed the furnace and the sample holder, were also raised by 2″ (50 mm) to allow the X-ray beam to irradiate the sample in the most uniform heat zone of the furnace. The entire camera could be evacuated through a 1″ vacuum port, and was subsequently continuously flushed with inert gas. The X-ray windows of the thermal radiation shield assembly consisted of nickel sheets.

The sample holder assembly, placed on a boron nitride stool within the quasi-cylindrical graphite furnace, consisted of two 0.005″ (0.13 mm) pyrolytic graphite sheets sandwiched between two graphite frames, each approximately 0.12″ (3 mm) thick with a vertical, machined window, 0.188″ (4.8 mm) wide and 0.625″ (16 mm) high, centered on the frames.

The choice of a container material for liquid metals is greatly influenced be thy compatibility of the liquid and the container. The choice of material is further limited since X-rays must be readily transmitted. In this particular sample holder assembly, the X-ray beam is transmitted through the windows in the frame but must still travel through the two pyrolytic graphite sheets and the sample, which is sandwiched between the sheets and suspended in foil form, by capillary action. A special cell was designed to contain the pure Mg sample in order to prevent evaporation. It consisted of a precision ground pyrolytic graphite frame surrounding the edge of the Mg sample. This frame in conjunction with the pyrolytic graphite windows prevented noticeable loss of Mg through evaporation.

B) Sample Preparation

Alloys of Cu and Mg with 49, 66.5 and 86 at. % Mg were prepared in the graphite sample holders directly in the high temperature camera. Foils of Cu and Mg were rolled to thickness ranging from 0.0002″ (5 μm) to 0.001″ (25 μm) for Cu and 0.001″ (25 μm) to 0.0055″ (0.4 mm) for Mg. The desired composition was achieved by sandwiching together foils of Cu and Mg of appropriate thickness, which were weighed before the measurements were made. The compositions were determined from the weights of the elements used. It was also necessary to maintain the total thickness of the foils close to the mean free path thickness. The mean free path thickness of the Cu-Mg alloy system for Mo radiation varied from 0.001″ (25 μm) for pure Cu to 0.005″ (0.13 mm) for Cu-90 at. % Mg, and 0.050″ (1.3 mm) for pure Mg.

In order to assure complete solution of the pure elements, Cu and Mg, both were cleaned in an appropriate acid etch. The Cu foils were first cleaned in a 50% HNO_3-50% distilled water solution, then in a 50% HCl-50% H_2O solution. They were then rinsed in triply distilled H_2O and dried in an argon atmosphere on ashless filter paper. The Mg foils were cleaned in a 5% H_2SO_4 solution, rinsed in distilled H_2O and dried on ashless filter paper in an Ar atmosphere. The foils were placed in the sample holder assembly and placed in the high temperature camera. After evacuation of the camera and subsequent flooding with a 80% Ar-20% H gas mixture, the furnace was turned on and the temperature was raised to approximately 50°C above the melting point of the alloy, at a rate of 300°C per minute. The rapid increase in temperature from room temperature to the melting point assured the mutual dissolution of the pure elements before surface oxidation of the foils could prevent it.

The Mg experiment was run at 700°C; the Cu-86 at. % Mg and the Cu-66.5 at. % Mg at 600°C; the Cu-49 at. % Mg at 685°C and the Cu at 1100°C. All of the experiments were carried out in a protective atmosphere of 80% Ar-20% H. Argon was used because the vapor pressure of Mg at its melting point of 651°C is relatively high. Loss of Mg through evaporation was not a problem when the alloy compositions of 66.5 and 86 at. %Mg were measured because the temperature at time of measurement was only 600°C. However, the pure Mg was run at 700°C and the vapor pressure of Mg at this temperature is 10 mm of Hg. This high vapor pressure required the use of the specially designed, "tight" sample holder.

No oxides of Cu or Mg were evident in the diffraction data during the runs and no material loss or composition change was evident by intensity change or change of peak maximum position of the first peak during the run.

C) Data Reduction and Analysis

Mo-Kα X-rays ($\lambda K\alpha = 0.711$ Å) were used as a radiation probe to measure the diffraction patterns of the liquid alloys.

In order to determine the $I(K)$ from the scattering pattern, the elastically scattered intensity had to be recorded. The Compton, or inelastic, scattering was quite small for Cu and was eliminated numerically. It was also eliminated numerically for Mg; however, its large values required great care to be taken in obtaining the scattering data.

The liquid alloys were measured in transmission in the graphite sample holder from $K = 0.8$ Å^{-1} to $K = 12.5$ Å^{-1}. The scattering from the graphite windows had to be considered. This required two experiments for every sample. One experiment was run with the liquid in its sample holder and the other was run with the sample holder empty. The scattered intensities used in the analysis were then taken from the smooth curve drawn through the experimental data points.

The sample holder scattering, $I_s(2\Theta)$, was corrected for absorption in the sample by the factor $A_s = \exp(-\mu t/\cos\Theta)$, where t is the thickness and μ is the linear absorption coefficient of the sample. The sample scattering, $I_f(2\Theta)$, corrected for sample holder scattering is then given by

$$I_f(2\Theta) = I_{meas.}(2\Theta) - I_s(2\Theta)A_s.$$

The value of μt of the sample was readily obtained by the attenuation of the straight-through beam by the sample, after lowering the intensity of the primary beam to manageable proportions with a 0.001″ tantalum foil acting as an absorber. The voltage was decreased so as not to excite $\lambda/2$ radiation which would also be scattered by the monochromator. The presence of $\lambda/2$ radiation would cause preferential absorption to take place in the sample or absorber and would lead to erroneous values for μt.

To obtain the coherent intensity per atom, $I_a(K)$, the sample intensity $I_f(2\Theta)$ was divided by the polarization factor (P) and the absorption factor (A_f) for X-rays in the sample. A_f is given by

$$A_f = (t/\cos\Theta)\exp[-(\mu t + \mu_s t_s)/\cos\Theta],$$

where μ_s and t_s are the absorption coefficient and thickness of the sample holder, respectively. The corrected intensity was then converted from 2Θ to $|K| = 4\pi(\sin\Theta)/\lambda$. This gave

$$I_a(K) = \beta(I_f(K)/PA_f) - I_a^{in.}(K),$$

where $I_a^{in.}(K)$ is the inelastic scattering and β is the normalization constant.

There are two common normalization procedures[1]; the high angle method[18] and the radial distribution function method[19]. In the investigation reported herein, the average of these two methods was used to obtain values for β.

III. Experimental Results

A) Interference Function (Structure Factor) of the Cu-Mg Alloys

The total interference functions $I(K)$ [Eq. (1)] of Cu, Mg and the Cu-Mg alloys are shown in Fig. 1, measured at the temperatures indicated in the diagrams.

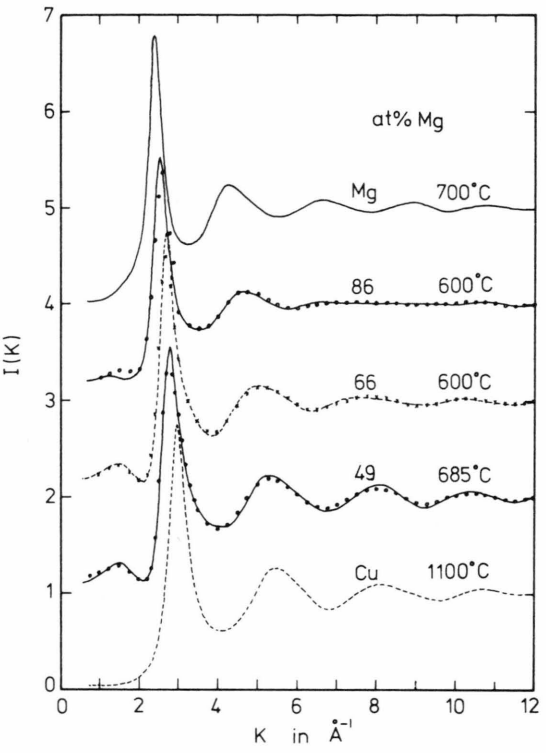

Fig. 1. Total interference function of liquid Cu, liquid Mg, and the liquid Cu-Mg alloys (open circles represent reproduction of the total interference functions from the weighted sum of the partial interference functions)

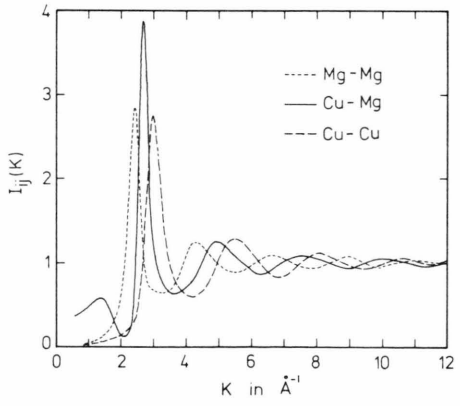

Fig. 2. The partial interference functions obtained from the total interference functions

Assuming that the partial interference functions $I_{ij}(K)$ [Eq. (3)] are independent of the relative abundance of the elements in the alloys, $I_{CuCu}(K)$, $I_{CuMg}(K)$ and $I_{MgMg}(K)$ were calculated by a least squares analysis

using $I(K)$ of the alloys and of pure Cu and Mg. Figure 2 shows $I_{ij}(K)$ obtained from $I(K)$.

B) Atomic and Radial Distribution Functions

The reduced atomic distribution functions $G(r)$ [Eq. (7)] are shown in Figure 3. The partial distribution functions, $G_{ij}(r)$ [Eq. (6)] were calculated by Fourier transformation of $I_{ij}(K)$, and are shown in Figure 4.

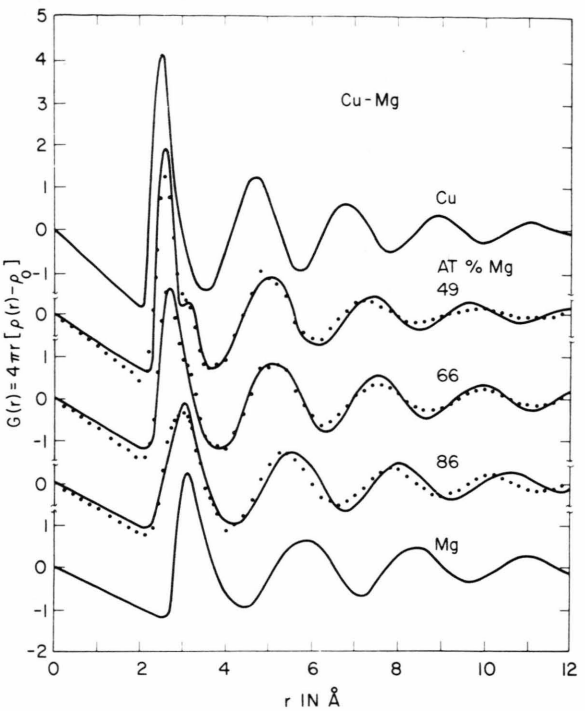

Fig. 3. Reduced total distribution functions of the liquid Cu-Mg alloys. The solid lines represent the Fourier transforms of $K[I(K)-1]$. The circles represent $\sum_i \sum_j w_{ij} G_{ij}(r)$.

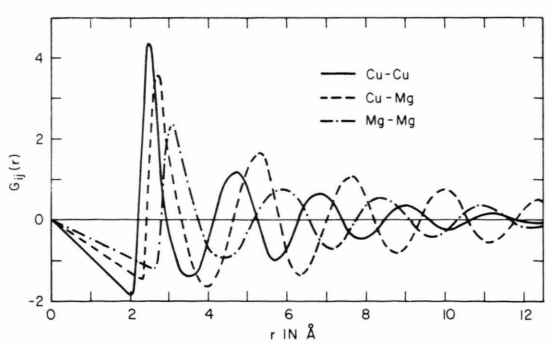

Fig. 4. The reduced partial distribution functions of the liquid Cu-Mg alloy system.

The position r_1, of the first peak maximum of $G_{ij}(r)$ is a measure of the interatomic separation between ij atomic pairs. The values of $(r_1)_{CuCu}$, $(r_1)_{CuMg}$ and $(r_1)_{MgMg}$ are given in Table I. It can easily be seen that $G_{Cu}(r)$ and $G_{Mg}(r)$ resemble $G_{CuCu}(r)$ and $G_{MgMg}(r)$, respectively. As is evident, $(r_1)_{Cu}$ and $(r_1)_{CuCu}$ are the same and $(r_1)_{Mg}$ and $(r_1)_{MgMg}$ are the same.

The radial distribution functions $4\pi r^2 \varrho(r)$ [Eq. (14)], which were obtained from $I(K)$ values with $K_{max} = 12.5$ Å^{-1}, are illustrated in Figure 5. The areas under

Table 1. Values of the position r_n in Å of the first and second peak maxima of $G_{ij}(r)$ and $G(r)$ for Cu-Mg alloys. Values of η (coordination number) evaluated from the radial distribution function.

Composition	r_1	r_2	η
CuCu	2.51	4.76	12.7
MgMg	3.10	5.76	11.9
CuMg	2.74	5.30	11.6
Cu—0 at. % Mg	2.51	4.75	12.7
—49 Mg	2.57	5.05	9.8
—66.5 Mg	2.69	5.20	9.5
—86 Mg	3.04	5.44	10.8
—100 Mg	3.10	5.75	11.7

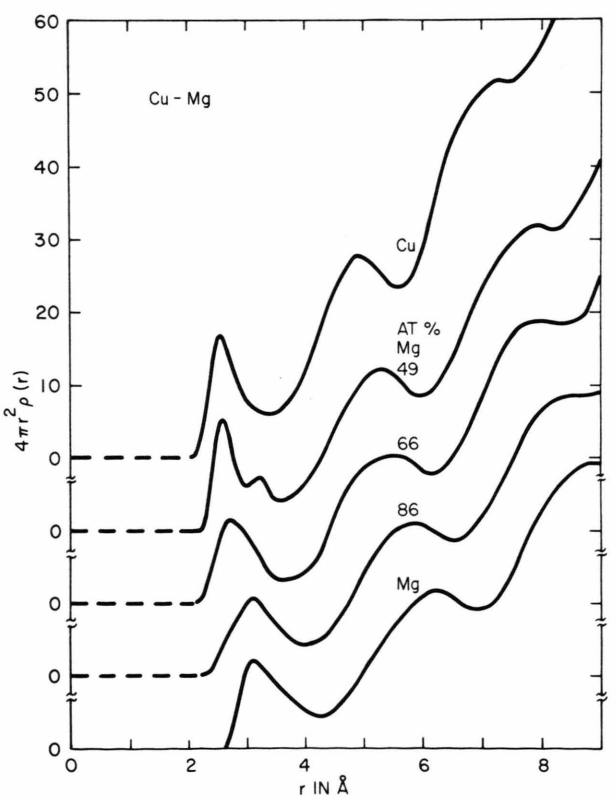

Fig. 5. Total radial distribution functions of liquid Cu-Mg alloys.

each first peak were determined to estimate the coordination number, η. There exists controversy[20,21] about the area under the first peak. It may be calculated either by making the $4\pi r^2 \varrho(r)$ curve symmetrical with respect to its rising part or by considering the minimum after the first peak as the cutoff point. Since there is doubt as to the validity of the assumption that the peak is indeed symmetrical, the second method was followed. The values of the coordination number, η are given in Table I.

IV. Discussion

In liquid Cu-Mg, the $I(K)$ show a premaximum at about 1.5 $Å^{-1}$, i.e., below the first main peak. The height of the premaximum depends on the concentration and appears to be strongest for the Cu-49 at. % Mg and Cu-66.5 at. % Mg alloys. The first few diffraction lines for compounds Cu_2Mg and $CuMg_2$ occur at 1.54 $Å^{-1}$, and 1.36, 1.42 and 1.71 $Å^{-1}$, respectively. The premaximum appears to be caused by atomic distances which are present in solid Cu_2Mg or $CuMg_2$. As can be seen in Fig. 1, only the height and not the position of the maximum changes with concentration. These facts indicate that atomic clusters similar to the solid compound Cu_2Mg or $CuMg_2$ must exist in the liquid state.

Similar results were found by Steeb and co-workers[2,4,5] in other Mg-base alloys. In the system AgMg[2], a premaximum was observed across the entire range of concentration and its height but not its position was a function of concentration. It was found that the intensity reached a maximum at the concentration of the $AgMg_3$ structure which exhibits crystalline peaks at 1.42, 1.59 and 1.75 $Å^{-1}$. The same results were found in the Pb-Mg[5] and Mg-Cd[6] and Mg-Sn[4] systems where the position of the premaximum was independent of concentration but its intensity changed with concentration, reaching a maximum at the concentration of the $PbMg_2$, Mg_3Cd and Mg_2Sn structures, respectively. No premaximum was observed in the Al-Mg system[3].

This evidence does not suggest the presence of crystalline planes in the liquid structure but it does suggest a local arrangement of Mg and Cu atoms which might give rise to this premaximum; and this local arrangement may be similar to that found in the Cu_2Mg or $CuMg_2$ compounds.

The $I_{ij}(K)$ of the liquid Cu-Mg alloy system were evaluated. In this alloy system, $I_{CuCu}(K)$ and $I_{MgMg}(K)$ resemble closely those observed in purre Cu and Mg, respectively, whereas $I_{CuMg}(K)$ shows a strong first peak and the premaximum which was observed in the alloys. This premaximum is an indication that a structure exists which shows a higher degree of order than observed in either pure Cu or pure Mg. As mentioned before, this premaximum might be related to local atomic arrangements which are similar to those found in the Cu_2Mg or $CuMg_2$ structures.

An interesting feature is that the values of $I_{CuMg}(K)$ and $I(K)$ of the alloys remain substantial as K approaches zero. This is small angle scattering which presumably reflects fluctuations in composition[12]. Even in pure liquid metals, $I(K)$ has a finite value as K approaches zero and this is a consequence of density fluctuations in the liquid. This value for most liquid metals and alloys, however, is of the order 0.01 to 0.02. In the case of liquid Cu-Mg alloys the values of $I(K)$ as K approaches zero range from 0.15 to 0.22. This is about ten to fifteen times greater than values of $I(K)$ observed in pure liquid metals. From this, the conclusion might be drawn that the high value of $I(K)$ as K approaches zero observed for Cu-Mg alloys is probably a result of compositional fluctuations present in the alloys. This fact, together with the observation of the premaximum in the alloys, suggests the presence of atomic clusters having local arrangements similar to those found in Cu_2Mg or $CuMg_2$. The composition of these clusters, being different from the surrounding material, would cause significant small angle scattering.

The real test concerning the usefulness of the X-ray partial functions rests in their ability to reproduce the total interference functions from which they were derived. As can be seen in Fig. 1, the weighted sum of the X-ray $I_{ij}(K)$ does not accurately reproduce $I(K)$. (The weighted sum of $I_{ij}(K)$ is represented by circles or crosses.) This could be an indication that $I_{ij}(K)$ are not independent of concentration across the entire range of concentration.

In order to further test the assumption of concentration independence of $I_{ij}(K)$, $G(r)$ of the alloys calculated from $I(K)$ using Eq. (6) and represented as solid curves in Fig. 3 were compared with $G(r)$, evaluated with Eq. (12) and represented with full circles in Figure 3. It is obvious from these figures that the agreement between the $G(r)$ curves is relatively poor. This same analysis, where $I_{ij}(K)$ and $G_{ij}(r)$ were derived from $I(K)$ of the alloys [assuming $I_{ij}(K)$ to be composition independent] was applied by WAGNER and coworkers to the Au-Sn[14], Ag-Sn[13] and Cu-Sn[16] alloy systems and also by LUKENS and WAGNER to the Ag-Cu system[22]. The agreement in those systems was good.

The poor agreement between $G(r)$ and $\sum_i \sum_j w_{ij} G(r)$ in the case of Cu-Mg could arise from the fact that $I_{ij}(K)$ are not independent of concentration or from the fact that w_{ij} [Eq. (10)] is strongly dependent of K or from both.

Let us look at the dependence of w_{ij} on K. The assumption that w_{ij} are independent of K cannot be responsible for the poor agreement between the weighted sum of $G_{ij}(r)$ and $G(r)$, because the actual K depend-

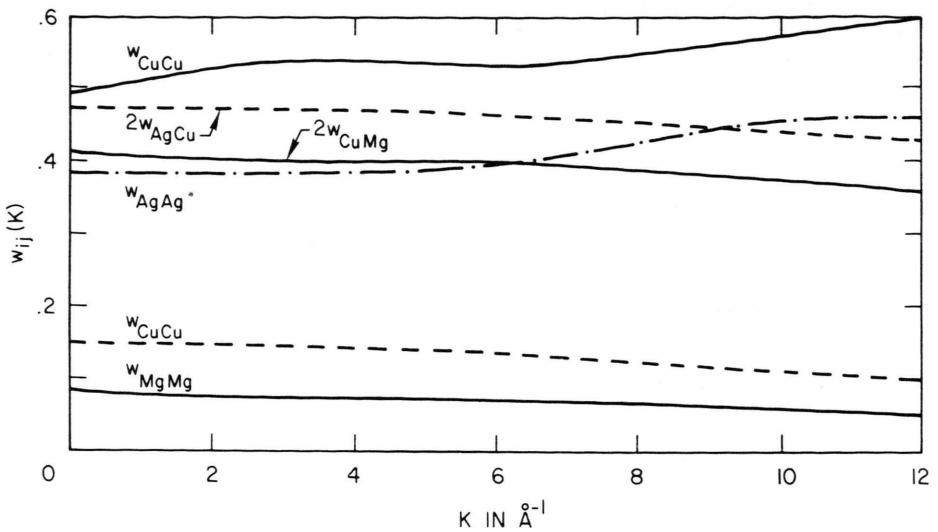

Fig. 6. The K dependence of the coefficients $w_{ij}(K)$ for Cu-49 at. % Mg, and for Ag-50 at. % Cu.

ence of w_{CuCu}, w_{CuMg} and w_{MgMg} for the alloy Cu-49 at. % Mg is only slightly greather tan that of w_{AgAg}, w_{AgCu} and w_{CuCu} for the alloy Ag-50 at. % Cu (Figure 6) Ag-Cu alloys represent a system wherein the assumption of concentration independence of $I_{ij}(K)$ proved to be valid. In addition, errors caused by the assumption that $w_{ij}(K)$ is independent of K would result in peak broadening or sharpening and not, as seen in Fig. 3, in peak position shifts.

The reason for the poor agreement must then be concentration dependence of the $I_{ij}(K)$, which makes it impossible for one set of three $I_{ij}(K)$ to characterize the entire concentration range.

Realizing that the functions $G_{ij}(r)$ were not uniquely determined, they were nevertheless used to evaluate the interatomic distances in the alloys. As shown in Table I, the values r_n of the maxima of $G_{CuCu}(r)$ appear at the same values of r as those of $G_{Cu}(r)$ and the values of r_n of the maxima of $G_{MgMg}(r)$ appear at the same values of r as those of $G_{Mg}(r)$. The size of the oscillations in $G_{CuMg}(r)$ is greater than it is in $G_{CuCu}(r)$ and $G_{MgMg}(r)$ and damps out less quickly. This fact indicates that the alloys might possess a higher degree of order than the pure elements.

It must be remembered that r_1 of the alloys really represent the positions of the first peak maxima of the weighted sum of the three $G_{ij}(r)$ and will, therefore, be strongly influenced by the weighting factors w_{ij}. The same argument holds true for the coordination number η. The coordination numbers of the Cu-Mg alloys as shown in Table I appear to decrease to a minimum, thus exhibiting a negative deviation from straight-line behavior, which might be considered as evidence for the existence of short-range-order in the liquid alloys[23].

VI. Summary and Conclusions

The scattering patterns of the Cu-Mg alloys cannot be interpreted as the weighted sum of $I_{ij}(K)$, derived from $I(K)$ of the pure elements and the alloys. This can be concluded from the fact that the Fourier transforms of $I_{ij}(K)$ yield $G_{ij}(r)$, which in turn do not reproduce $G(r)$, the transforms of $F(K) = K[I(K) - 1]$, of the alloys.

The premaximum in $I(K)$ of the alloys might be an indication that local atomic arrangements similar to those found in the Cu_2Mg or $CuMg_2$ compounds are present in the liquids.

References

1 C.N.J. Wagner; Liquid Metals, Chemistry and Physics, Beer, Sylvan (ed.), Marcel Dekker, New York 1972, Chapter 6, p. 257.

2 S. Steeb and R. Hezel; Z. Metallkde. **57**, 374 (1966).

3 S. Steeb and S. Woerner; Z. Metallkde. **56**, 771 (1965).

4 S. Steeb and H. Entress; Z. Metallkde. **57**, 803 (1966).

5 S. Steeb, D. Dilger and J. Höhler; Phys. Chem. Liquids **1**, 235 (1969).

6 A. Boos, S. Steeb and D. Godel; Z. Naturforsch. **27a**, 271 (1972).

7 P. Debye and A.M. Bueche; J. Appl. Phys. **20**, 518 (1949).

8 C.N.J. Wagner; Advances in X-Ray Analysis **12**, 50 (1969).

9 C.J. Pings and J. Waser; J. Chem. Phys. **48**, 3016 (1968).

[10] R. KAPLOW, S.L. STRONG and B.L. AVERBACH; Local Atomic Arrangements, Studied by X-Ray Diffraction, COHEN, J.B. and HILLIARD, J.E. (eds.), Gordon and Breach Science Publishing Company, New York 1966, p. 159.

[11] D.T. KEATING; J. Appl. Phys. **39**, 923 (1963).

[12] J.E. ENDERBY, D.M. NORTH and P.A. EGELSTAFF; Phil. Mag. **14**, 961 (1966).

[13] N.C. HALDER and C.N.J. WAGNER; J. Chem. Phys. **47**, 4385, (1967).

[14] C.N.J. WAGNER, N.C. HALDER and D. NORTH; Phys. Letters **25A**, 663 (1967).

[15] H.F. BÜHNER and S. STEEB; Z. Naturforsch. **24a**, 428 (1969).

[16] D.M. NORTH and C.N.J. WAGNER; Phys. Chem. Liquids **2**, 87 (1970).

[17] D.M. NORTH and C.N.J. WAGNER: J. Appl. Crystallography **2**, 149 (1969).

[18] N.S. GINGRICH; Rev. Mod. Phys. **15**, 90 (1943).

[19] K. FURUKAWA; Rep. Prog. Phys. **25**, 395 (1962).

[20] K. FURUKAWA, B.R. ORTON, J. HAMOR and G.I. WILLIAMS; Phil. Mag. **8**, 141 (1963).

[21] C.J. PINGS; Physics of Simple Liquids, H.N.V. TEMPERLY, J.S. ROWLINSON, and G.S. RUSHBROOKE, (eds.), North-Holland Publishing Company, Amsterdam 1968, p. 388.

[22] W.E. LUKENS and C.N.J. WAGNER; to be published (see W.E. LUKENS' Ph. D. Thesis, Yale University, New Haven, Connecticut 1971).

[23] S. STEEB and R. HEZEL; Z. Phys. **191**, 398 (1966).